

PAPER • OPEN ACCESS

## Numerical modelling of structural behaviour of URM panels strengthened with cement matrix composites

To cite this article: D A Ghiga *et al* 2019 *IOP Conf. Ser.: Mater. Sci. Eng.* **591** 012037

View the [article online](#) for updates and enhancements.

# Numerical modelling of structural behaviour of URM panels strengthened with cement matrix composites

**D A Ghiga, N Taranu, D Ungureanu, DN Isopescu, MC Scutaru and I Hudisteanu**

”Gheorghe Asachi” Technical University of Iasi, Faculty of Civil Engineering and Building Services

E-mail: danghiga@hotmail.com

**Abstract:** Unreinforced masonry (URM) structures represent a large share of the dwelling stock, traditional industrial buildings and historical heritage of mankind. Most of the URM structures have been built with little or, in some cases, no seismic provisions. In order to overcome this drawback, the application of external reinforcement layers, especially those made of composites, to improve the structural behavior of masonry structures has been a research focus area during the past decades.

The aim of this paper is to propose and assess a simplified and accepted Finite Element (FE) modelling strategy to simulate the diagonal compression test of the URM walls strengthened with glass fibre meshes embedded in a cement-based mortar. In the case of masonry walls strengthened with composites reinforced with glass fibre meshes, both the masonry material model and the modelling and the meshing of the composite strengthening system need to be addressed by taking into account the complex phenomena that characterise the bond interaction between the glass fibre mesh, mortar and the masonry support. The FE analyses were developed with reference to the experimental tests available in the current literature and, according to the preliminary outcomes of an experimental program which is currently under development at the Faculty of Civil Engineering and Building Services, Iasi.

## 1. Introduction

Unreinforced masonry (URM) structures represent a significant part of the existing building stock, belonging to the World cultural and Historical heritage. The design philosophies of these structures were focused, in most of the cases, only on the gravity loading and thus, a large share of these buildings is potentially vulnerable to seismic actions [1]. Therefore, it is needed to improve their seismic performances by strengthening. According to Triantafillou, the strengthening methods can be classified into: external reinforcement consisting in the application of either fibre reinforced polymer (FRP) systems or textile reinforced mortar (TRM) jacketing, injection, post tensioning and traditional retrofitting [2]. Among these, the TRM jacketing method has demonstrated an improved compatibility in terms of bonding with various masonry substrates mainly due to the peculiar characteristics of the cementitious mortar matrix. Also, previous numerical and experimental studies show that the URM walls strengthened by TRM jacketing reached higher shear strength and pseudo-ductility, when compared to the ones strengthened through other similar methods [3-5].

The design of the TRM systems for strengthening the existing URM structures requires suitable structural analysis tools. So far, macro-numerical finite element (FE) models have been generally accepted for the numerical analysis of the URM strengthening systems [6]. In the case of the TRM



strengthening systems, the stresses usually concentrate into narrow areas along the faces of the transversal connectors. The macro-numerical models are unable to account for the micro-mechanical characteristics at the interface levels; therefore, these types of stress concentrations cannot be distinguished. On the other hand, more recent modelling strategies, such as the detailed micro-numerical, allows for identifying and monitoring all the components of the stress-strain state of any type of strengthening systems of URM [6-8]. In this approach, the masonry units, the mortar joints and the constituents of the strengthening system are modelled separately as continuum elements and the interfaces between all the components are represented as discontinuous elements. It can be noted that the micro-numerical models are designed to account for all the components of the physical models, the corresponding materials and their characteristics, thus reflecting the realistic behaviour of the URM structures strengthened with TRM. Moreover, due to the specific features of this modelling strategy, the FE micro-models can be adapted to simulate various laboratory tests.

In this study, a detailed micro non-linear 3D model has been developed to simulate the diagonal compression test of URM walls strengthened with glass fibre meshes embedded in a thixotropic cement-based mortar. Also, for comparison purposes, a benchmark URM wall was modeled without the TRM strengthening system. The numerical simulations provided results in good agreement with the ones obtained by previous experimental tests, available in the current literature.

## **2. Numerical modelling**

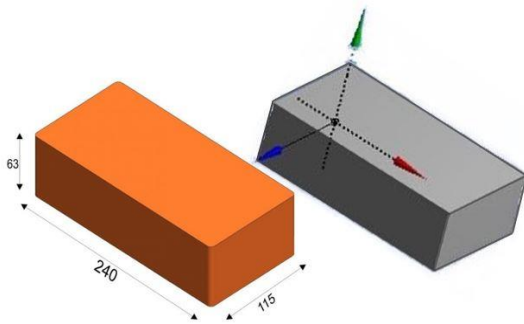
The numerical analyses presented in this paper were carried out using the commercial, multi-purpose finite element software Ansys. This software, widely used particularly for research studies, contains a large engineering data base concerning both material models and finite elements. In particular, in case of nonlinear analyses, the available numerical models allow to account for the distinct behaviour of materials in compression and tension, as well as for the influence of existing pre-damages. Moreover, the Ansys software contains a wide library of different constitutive laws, including linear / multi-linear, parabolic and exponential, which enables an exhaustive modelling of the softening behavior of various materials in compression and tension [9-11].

### *2.1. Model definition*

To simulate the in-plane behaviour of the URM models strengthened with TRM under diagonal compression test, a micro non-linear 3D model was conceived. For this numerical model, the detailed masonry structure was considered, and the bricks and the mortar were modelled separately. The masonry units – mortar joints interfaces were modelled by contact/interface elements.

#### *2.1.1. Material properties*

Masonry is an anisotropic composite material made with masonry units and mortar. The mechanical models developed to characterise the structural behaviour of masonry structures falls under the category of no-tension material models. In particular, the URM walls are considered to be incapable of withstanding significant tensile stresses and, consequently, they behave like a linear elastic material when subjected to compressive stresses. However, based on the elastic and the mechanical properties of the constitutive materials, the mechanical model and by default, the numerical one, may vary from linear-elastic to elasto-plastic material models. The URM walls analysed in this study were considered to be manufactured with brick units fabricated by Wienerberger. The geometry of the masonry units, the assessed 3D model and the physical and mechanical properties, as determined and provided by the manufacturer, are presented in figure 1 [12].



Characteristics	Unit
Mass	3.25 kg
Density	1850 kg/m <sup>3</sup>
Compressive strength	15 MPa

**Figure 1.** Wienerberger brick units. Physical and mechanical properties [12].

The masonry panels were considered to be built with a mortar (M 50 Z), composed of Portland cement, lime and sand in the proportion and quality commonly used in the existing traditional Romanian URM buildings. In the case of masonry walls subjected to diagonal compression, a combined state of shear and compression occurs in the joints and hence, the mechanical properties of both the masonry units and mortar, in compression and shear are necessary in the adopted numerical models. The values of these material properties were provided by the manufacturers. Instead, realistic values of these parameters were deduced both from experimental tests and from theoretical considerations (table 1) [6, 13-17].

**Table 1.** Properties of the constituents of the URM walls [6, 13-17].

Properties	Brick	Mortar
Elasticity modulus, E (MPa)	2000	4000
Poisson's ratio, $\nu$	0.16	0.21
Ultimate tensile strength, $f_t$ (MPa)	1.46	0.66
Ultimate compressive strength, $f_c$ (MPa)	15	4.46

The masonry strengthening system analysed in this study consists in a high strength, two-component, cement-based mortar (Planitop HDM Maxi) [18] reinforced with a glass fibre mesh (Mapegrid G 220) [19]. This TRM was applied on both faces of the URM panels and the structural connections between the strengthening system and the supports were achieved by means of through-wall, glass fibre cords (MapeWrap G FIOCCO) [20] impregnated with a polyester resin (Mapefix PE Wall) [21]. Most of the necessary material properties were determined and provided by the manufacturer (tables 2-5). However, since no information on the Poisson's ratio and the fracture energy were available, these properties were taken from the literature. The appropriate value of the fracture energy characterizing the constitutive law of the glass fibre mesh has been calibrated through fitting analysis of the existing experimental results. Thus, the values of the fracture energy in compression and tension were namely equal to 8N/mm and 0.1N/mm, while the Poisson's ratio was taken as 0.3, in agreement with the literature data.

**Table 2.** Planitop HDM Maxi mortar. Physical and mechanical properties [18].

Properties	Unit
Density of wet mix	1850 kg/m <sup>3</sup>
Adhesion to masonry	2 MPa
Compressive strength	25 MPa, determined at 28 days
Tensile strength	8 MPa, determined at 28 days
Compressive modulus of elasticity	10000 MPa, determined at 28 days

**Table 3.** Mapegrid G220 glass fibre mesh. Physical and mechanical properties [19].

Properties	Unit
Weight	225 g/m <sup>2</sup>
Mesh size	25 x 25 mm
Density of fibres	2500 kg/m <sup>3</sup>
Tensile strength	45000 N/m
Modulus of elasticity	72000 MPa
Elongation at failure	1.8 %

**Table 4.** MapeWrap G FIOCCO. Physical and mechanical properties [20].

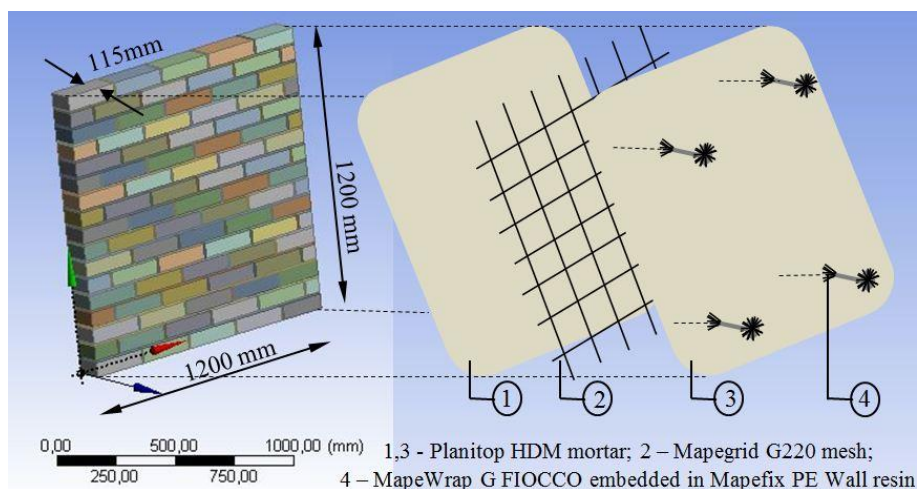
Properties	Unit
Density	2620 kg/m <sup>3</sup>
Tensile strength	2.56 MPa
Modulus of elasticity	80.70 MPa
Elongation at failure	3 %

**Table 5.** Mapefix PE Wall. Physical and mechanical properties [21].

Properties	Unit
Density (mixed)	1690 kg/m <sup>3</sup>
Compressive strength	68 MPa
Tensile strength	30 MPa
Modulus of elasticity in compression	6105 MPa

### 2.1.2. Modelling strategy

The proposed numerical model used to study the in-plane shear behaviour of strengthened URM walls is based on the 3D micro modelling approach. The nominal dimensions of the masonry units, the thickness of the joints and the boundary conditions were modelled to accurately represent the characteristics of the experimental panels. The components of the 3D models are illustrated in figure 2.

**Figure 2.** Components of the 3D model.

For this modelling strategy, the bricks and the mortar were modelled using the SOLID187 tetrahedron finite elements (figure 3(a)) [22]. These model components consist of higher-order 3D – elements defined by 10 nodes, each of them enabling 3 degrees of freedom. Also, these types of finite elements are characterised by quadratic displacement behaviour with large deflection and strain capabilities. The TRM components and the transversal connectors were modelled using the SHELL 63 finite element, since these types of components have both bending and membrane capabilities (figure 3(b)) [22]. Furthermore, the 3D models were conceived so as to account for 3 interface levels (brick-mortar, brick-TRM and mortar-TRM). For this purpose, bonded contact elements of type CONTA174 were defined at each interface level (figure 3(c)) [23]. These types of elements may accurately simulate the interface delamination, since they were modelled to allow the contact separation for the brick-TRM and mortar-TRM interfaces.

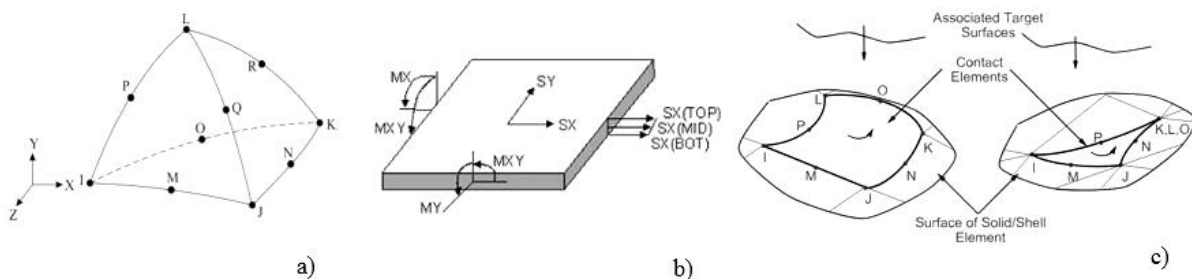


**Figure 3.** (a) SOLID187 finite element, (b) SHELL 63 finite element, (c) CONTA174 finite element \*i, j, k, l, m, n, o, p, q, r – nodes;  $M_{X, Y, XY}$  – bending moments;  $S_{X, Y}$  – displacements. Figure adapted from [24].

The masonry units were modelled as being linear elastic isotropic materials and the plasticity properties were assessed to the mortar layers. The structural performance of the mortar is capable to account for the overall non-linear behaviour of the masonry module. Moreover, by applying this modelling strategy it is ensured that the dominant failure mode will be developed in a characteristic pattern, which consists of a continuous diagonal crack along the bed and head joints. The mortar was modelled as an elastoplastic material, using the Drucker-Prager formulation [25]. According to this yield criterion formulation, the material model is defined by a characteristic domain of yield stresses. In the space of main stresses, this domain consists of a cone whose axis matches the main (space) diagonal of the principal stresses ( $\sigma_1, \sigma_2, \sigma_3$ ) coordinate system (figure 4). The material starts to deform plastically, when the yield surface is reached. Upon further loading, the deformation produces plastic flow.

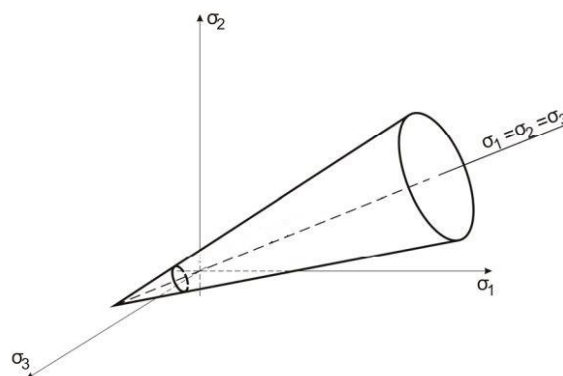


**Figure 4.** Drucker-Prager failure domain \*Figure adapted from [26].

The interface levels were defined by an Augmented Lagrange formulation. This type of contact formulation is used when the penetration between the contact and the target bodies is detected and controlled at a specific level [27]. The penetration points were assessed to the masonry units and to the mortar layers by applying the integration point detection. This is an iteration method which provides significant more detection points when compared to the basic nodal detection method.

Furthermore, in this study, the complete test specimens were modeled, and the symmetries were not exploited to facilitate the modeling of the boundary conditions. Additionally, the parameters of position and connectivity were defined for each node to match the specimen geometric configurations (figures 5, 6).

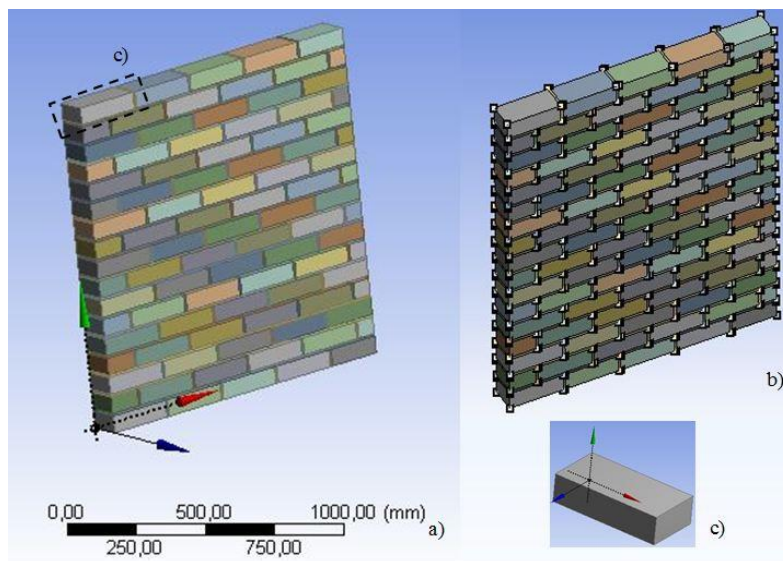


**Figure 5.** 3D model of URM wall.

a) URM wall, b) parameters of position and connectivity, c) masonry unit

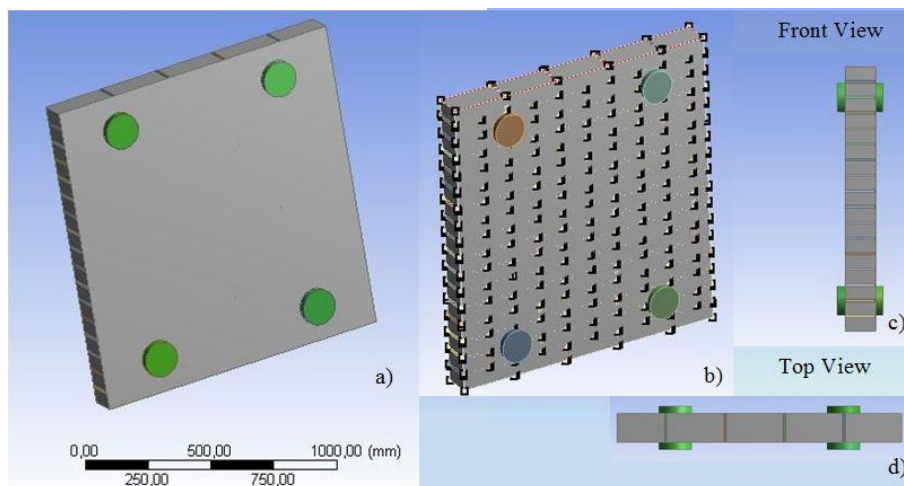


**Figure 6.** 3D model of URM wall strengthened with TRM.

a) strengthened URM wall, b) parameters of position and connectivity, c) Front view of the panel, d) Top view of the panel

The mesh size was kept different for bricks, mortar layers, TRMs and transversal connectors, as per their geometrical configurations. For the masonry units, the maximum mesh size was chosen as 15

mm; for the mortar layers and transversal connectors, the mesh size was kept as 2 mm; for the TRM, the maximum size of the mesh was set to 80 mm (figure 7).

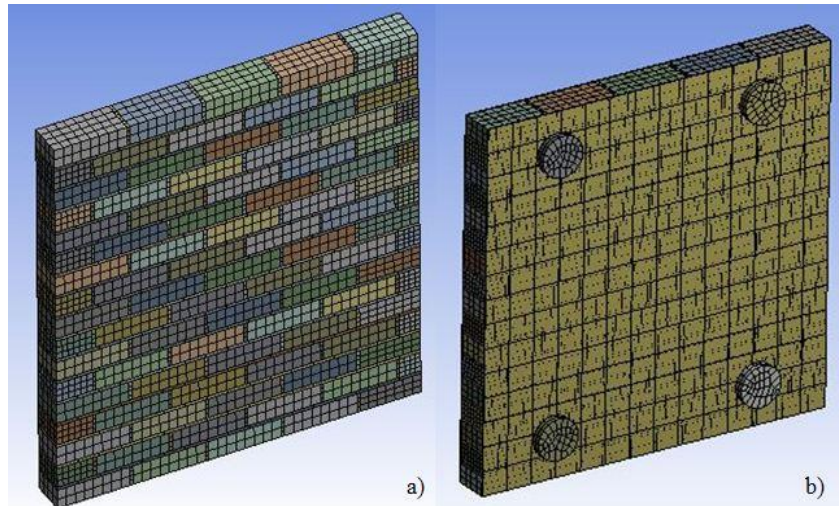


**Figure 7.** Mesh details of a) URM wall, b) URM wall strengthened with TRM.

The nonlinear models were analysed using a method based on several iterative series of linear approximations [28]. This approach, also referred to as the Newton-Raphson Method, is structured on three levels (residual level, convergence level and equilibrium level). Within the first level, the differences between the external and the internal forces are evaluated, and the results are recorded as “residuals”. In the second stage, several iterations are performed until the values of the “residues” become acceptably small (less than the criterion). When the “convergence” is achieved, the solution is considered to be in “equilibrium”, within an acceptable tolerance.

The Newton-Raphson method was applied by gradually increasing the load until the convergence criterion was achieved. In addition, several sub-steps were defined to divide the load step whenever required. The final step, corresponding to the ultimate load (at the end of the elastic branch), was established for the stage when a sudden and abrupt change in displacement occurred (the convergence criterion was not satisfied).

### 3. Results and discussions

The shear structural performance of the strengthened panel was evaluated and compared with respect to the results obtained for the URM module. Figures 8 and 9 show the shear stress distributions for both numerical models.

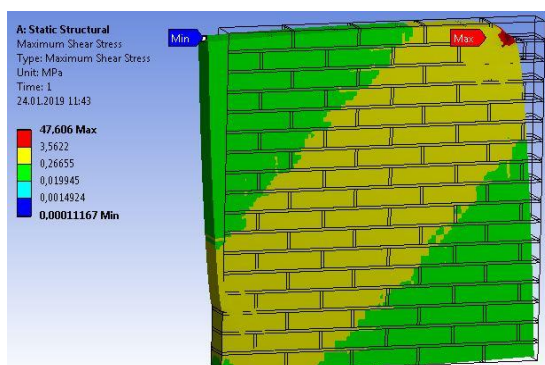


**Figure 8.** Shear stress distribution map for the un-strengthened URM panel.

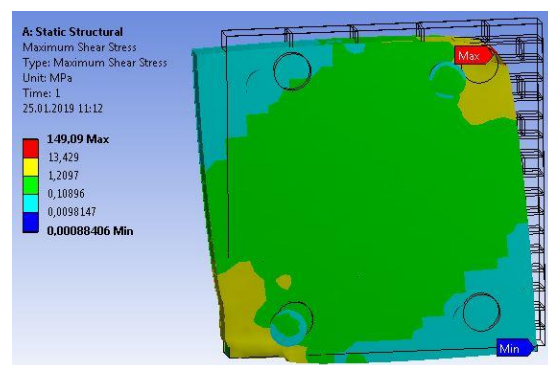


**Figure 9.** Shear stress distribution map for the URM panel strengthened with TRM.

As it can be observed, in the case of the strengthened panel, the shear resistance capacity is significantly increased. The ultimate load increases from 28kN to almost 100kN with respect to the un-strengthened URM module. Additionally, the maximum shear stresses determined for the URM modules strengthened with TRM are almost 3 times higher compared to the ones determined for the un-strengthened module.

The transversal connectors that were considered in this study provided enough fastening and bonding capacity to avoid the interface debonding between the masonry walls and the TRM system. At the same time, the fan angle ( $360^\circ$ ) and the radius (60mm) ensure sufficient area for the distribution of the stresses; therefore, no significant stress concentrations were identified.

During the numerical analyses it was found that for the un-strengthened URM module, cracks may develop at early stages of loading. Upon increasing the loading, the crack pattern tended to concentrate in a diagonal shear band. Although this behaviour was common to both the un-strengthened and the strengthened models, in the second case the pair of initial crack paths that emerge from the opposite corners of the model did not unite. This failure mechanism is also illustrated by the shear stresses distribution maps (figures 8, 9), where the concentration of stresses can be easily observed in a large diagonal band with peak stresses at the top-right and bottom-left corners. Moreover, the compressive and the shear strengths at these locations were completely exhausted, which indicates that failure was governed by the mortar layer. This result is in reasonable agreement with experimental evidences [6].

Moreover, the numerical models led to acceptable results regarding the stiffness characteristics in the post-peak stage. However, the un-strengthened model showed a slightly more pronounced reduction in stiffness compared to the strengthened one. In particular, at a drop in force of 10% on the softening branch, the total displacement was approximately the same for both models, while at a drop of 20%, the displacements stabilized at 2.17mm for the strengthened model and 1.83mm for the un-strengthened model (figures 10, 11).

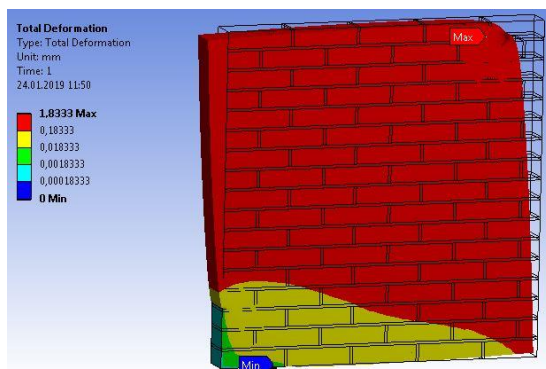


**Figure 10.** Displacement map for the un-strengthened URM panel.

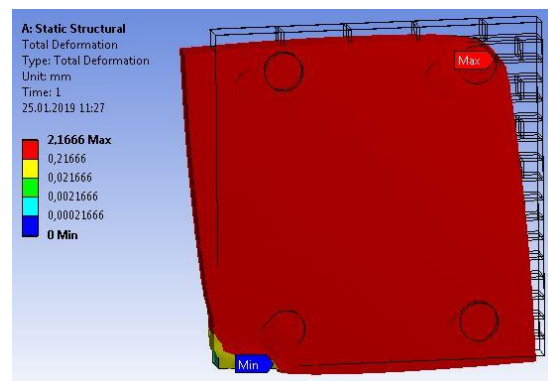


**Figure 11.** Displacement map for the URM panel strengthened with TRM.

#### 4. Conclusions

Several modelling aspects related to a finite element modelling strategy designed to simulate the diagonal compression test of the URM walls strengthened with TRM were analysed and discussed in this paper. The structural concept, the geometrical configuration and the materials were selected in accordance with the specifications of the manufacturer of the TRM strengthening system. For each type of material (including both the components of the masonry wall and of the TRM system) distinct finite element models were assessed. The boundary conditions and the parameters of position and connectivity were modelled to accurately represent the characteristics of the experimental panels. Furthermore, the final micro non-linear 3D models were designed to account for the distinct behaviour of materials in compression and tension, as well as for their constitutive laws and softening behaviour.

The numerically determined results confirmed the efficiency of shear strengthening the URM walls using TRM, particularly for those strengthened on both faces. Nonetheless, in order to draw reliable and broad conclusions, these results should be validated through more extensive experimental tests.

Conducting more laboratory experimental investigations will be useful in order to study the influence of different strengthening variables on the structural behavior of the masonry walls. These variables may include the type and the spacing of the fibre grids, the type of the matrix and the mean thickness of the TRM system. Additionally, other special issues, such as the use of transversal connectors between the TRM system and the masonry substrate, in order to further explore the possibility of improvement in performance of the strengthened URM walls using TRM could be addressed.

## 5. References

- [1] Institutul National de Statistica (National Institute of Statistics) 2017 *Fondul national de locuinte (National Housing Fund) 2016*
- [2] Triantafillou T 2016 *Strengthening of existing masonry structures: Concepts and structural behavior (Textile Fibre Composites in Civil Engineering vol 1)* (Sawston, UK: Woodhead Publishing) chapter 15 pp 361–374
- [3] Kouris L A S and Triantafillou T C 2018 State of the art on strengthening of masonry structures with textile reinforced mortar (TRM) *Construction and Building Materials* **188** 1221-1233
- [4] Shabdin M, Zargaran M and Attari N K A 2018 Experimental diagonal tension (shear) test of Un-Reinforced Masonry (URM) walls strengthened with textile reinforced mortar (TRM) *Construction and Building Materials* **164** 704-715
- [5] Carozzi FG, Poggi C, Bertolesi E and Milani G 2018 Ancient masonry arches and vaults strengthened with TRM, SRG and FRP composites: Experimental evaluation *Composite Structures* **187** 466-480
- [6] Khan H A, Nanda R P and Das D 2017 In-plane strength of masonry panel strengthened with geosynthetic *Construction and Building Materials* **156** 351-361
- [7] Bernat-Maso E, Gil L and Roca P 2015 Numerical analysis of the load-bearing capacity of brick masonry walls strengthened with textile reinforced mortar and subjected to eccentric compressive loading *Engineering Structures* **91** 96-111
- [8] Lucchesi M, Padovani C, Pasquinelli G and Zani N 2008 *Masonry constructions: Mechanical models and Numerical applications* (Berlin: Springer)
- [9] *Ansys Mechanical User's Guide* available on-line at: [https://www.sharcnet.ca/Software/Ansys/16.2.3/en-us/help/wb\\_sim/ds\\_Home.html](https://www.sharcnet.ca/Software/Ansys/16.2.3/en-us/help/wb_sim/ds_Home.html), accessed on: 14.11.2018
- [10] Ungureanu D, Taranu N, Lupasteanu V, Isopescu D N, Oprisan G and Mihai P 2018 Experimental and numerical investigation of adhesively bonded single lap and thick adherents joints between pultruded GFRP composite profiles *Composites Part B: Engineering* **146** 49-59
- [11] Ungureanu D, Taranu N, Isopescu DN, Lupasteanu V, Mihai P and Hudisteanu I 2017 Analytical and numerical study of adhesively bonded composite pultruded elements *Rev Rom Mat* **47** 252-266
- [12] Wienerberg solid brick clay masonry unit - Technical data sheet 2018.
- [13] Shabdin M, Zargaran M and Attari N K A 2018 Experimental diagonal tension (shear) test of Un-Reinforced Masonry (URM) walls strengthened with textile reinforced mortar (TRM) *Construction and Building Materials* **164** 704-715
- [14] Fagone M and Ranocchiai G 2018 Experimental investigation on out-of-plane of masonry panels strengthened with CFRP sheets *Composites Part B* **150** 14-26
- [15] Gattulli V, Lampis G, Marcari G and Paolone A 2014 Simulations of FRP reinforcement in masonry panels and application to a historic façade *Engineering Structures* **75** 604-618

- [16] Grande E, Imbimbo M and Sacco E 2013 Finite element analysis of masonry panels strengthened with FRPs *Composites: Part B* **45** 1296-1209
- [17] Lee D and Shin A H C 2016 Finite element study on the impact responses of concrete masonry unit walls strengthened with fiber-reinforced polymer composite materials *Composite Structures* **154** 256-268
- [18] *Planitop HDM Maxi* – Technical data sheet 2018
- [19] *Mapegrid G 220* – Technical data sheet 2018
- [20] *MapeWrap G FIOCCO* – Technical data sheet 2018
- [21] *Mapefix PE Wall* – Technical data sheet 2018
- [22] Nelson T and Wang E 2004 *Reliable FE-Modeling with ANSYS* (Ansys support data base) available on-line at: <https://support.ansys.com/staticassets/ANSYS/staticassets/resourcelibrary/confpaper/2004-Int-ANSYS-Conf-24.PDF> accessed on: 08.11.2018
- [23] *Ansys courses* available on-line at: [http://www2.me.rochester.edu/courses/ME204/nx\\_help/index.html#uid:xid457126](http://www2.me.rochester.edu/courses/ME204/nx_help/index.html#uid:xid457126), accessed on: 18.01.2019
- [24] *Ansys courses* available on-line at: [https://www.sharcnet.ca/Software/Ansys/15.0.7/en-us/help/ans\\_thry/thy\\_el174.html](https://www.sharcnet.ca/Software/Ansys/15.0.7/en-us/help/ans_thry/thy_el174.html), accessed on: 09.01.2019
- [25] Bennet K C, Regueiro R A and Luscher D J 2018 Anisotropic finite hyper-elastoplasticity of geomaterials with Drucker-Prager/Cap type constitutive model formulation *International Journal of Plasticity* doi.org/10.1016/j.ijplas.2018.11.010
- [26] Cervera M, Chiumenti M, Benedetti L and Codina R 2015 Mixed stabilized finite element methods in nonlinear solid mechanics. Part III: Compressible and incompressible plasticity *Computer Methods in Applied Mechanics and Engineering* **285** 1-31
- [27] *Ansys courses* available on-line at: [https://www.sharcnet.ca/Software/Ansys/17.0/en-us/help/wb\\_sim/ds\\_contact\\_theory.html](https://www.sharcnet.ca/Software/Ansys/17.0/en-us/help/wb_sim/ds_contact_theory.html), accessed on: 15.12.2018
- [28] *Ansys courses* available on-line at: [https://www.sharcnet.ca/Software/Ansys/16.2.3/en-us/help/ans\\_thry/thy\\_tool10.html](https://www.sharcnet.ca/Software/Ansys/16.2.3/en-us/help/ans_thry/thy_tool10.html), accessed on: 18.01.2019